SATBAYEV UNIVERSITY

Engineering Journal of Satbayev University

Volume 146 (2024), Issue 1, 7-14

https://doi.org/10.51301/ejsu.2024.i1.02

Enhanced damping properties of novel Cr-Ni-V steels with ceramical-metal nanostucture TiN-Cu coatings

R.Zh. Abuova[1*], A. Bondarev[2], G.A. Burshukova[3]

[1]*International education corporation, Almaty, Kazakhstan*
[2]*University of Limerick, Ireland*
[3]*Satbayev University, Almaty, Kazakhstan*

**Corresponding author: ryskena@mail.ru*

Abstract. The paper investigates novel steel compositions, alloyed with Cr, Ni, and V, exhibiting improved damping properties. Additionally, it proposes a surface coating method to further enhance damping capabilities. Furthermore, the study presents findings on structure and phase formation processes in (TiN)-Cu coatings, deposited via vacuum-arc deposition on EO5 steels substrates. The coating fracture exhibits signs of ductile fracture, accompanied by the formation of fibrous-banded pits on the fracture surface. Scratch tests reveal shear stresses are presumed to be the primary cause of delamination. With increased load, coatings primarily fail along the scratch edge, indicating significant involvement of compressive and tensile stresses. This behavior is attributed to the nanocomposite structure, which hinders crack propagation and allows to maintain ductility. TEM analysis reveals a nanocomposite structure, with electron diffraction confirming the presence of titanium nitride δ-TiN crystallites. No crystallographic texture is observed in the coatings. The coatings significantly influence the internal friction amplitude dependence characteristics. The intricate microstructure, including and internal interfaces, contributes to complex damping properties. Additional damping mechanisms occur at grain interfaces and at the coating-substrate boundary.Further damping mechanisms are incorporated at the interfaces of individual grains and particles and at the interphase interaction boundary in the coating-base system, in addition to the internal damping mechanisms that occur in the coating itself and the substrate independently.

Keywords: *nanostructure, damping, dislocation, microstructure, noise, vibration, sound level meter.*

1. Introduction

The strategic development of mechanical engineering, associated with technical rearmament, increased labor productivity, and the quality of machine part processing, is largely determined by the implementation of technologies based on automatic lines and flexible manufacturing systems, the reliability of which is conditioned by increased requirements for cutting tools in terms of strength, wear resistance, economic indicators, and the significant role of mechanical noise of impact origin. Noise and vibration in production are harmful and dangerous factors that negatively affect human health. It should be noted that these factors can confidently be called relatives, since they all have a mechanical oscillatory nature of origin. Diseases of the auditory organs (neurosensory hearing loss), musculoskeletal system (vestibular syndrome, polyneuropathy of the upper and lower limbs), cardiovascular system (angiodystonic syndrome) can be caused by prolonged work under the influence of vibroacoustic factors with levels exceeding hygiene standards for workplaces. Occupational diseases related to vibroacoustics account for more than 53% of professional disability losses worldwide. To reduce the noise level at its source, it is necessary to replace impact processes with non-impact ones, replace metallic materials with non-metallic ones, and a number of other methods that effectively combat noise levels [1-8].

The damping capacity of metallic materials is characterized by a combination of acoustic and physico-mechanical characteristics, such as sound pressure level, sound attenuation rate, internal friction, specific electrical resistance, density, shear modulus, and Young's modulus, as well as a number of metallographic features. In the present study, a series of experiments aimed at establishing the relationships between structurally sensitive factors and microstructure with the optimization parameter - the sound level of structural low-alloy steels, the composition of which was determined by the experiment design matrix, were conducted. The selection of nickel, chromium, and vanadium as alloying elements in iron-carbon alloys is explained as follows. As the analysis of works [9-12] showed, alloys with enhanced damping properties contained chromium, nickel, and vanadium as alloying elements. It should be noted that nickel is one of the most abundant elements on Earth (0.09%) and is widely used in iron-based alloys with high damping properties. Nickel additions from 2% to 4% also affect the damping properties of alloys.

The choice of chromium as an alloying element is explained by its wide application in high-damping alloys. Chromium additions to other metals significantly alter their properties and create opportunities for obtaining a wide range of valuable materials. By slightly strengthening ferrite, chromium does not decrease its viscosity, and it is known to be present in more than 3.000 steels and alloys [13].

ryskena@mail.ru; abondarev88@gmail.com; gzzi@mail.ru
Engineering Journal of Satbayev University. eISSN 2959-2348. Published by Satbayev University

Vanadium belongs to the elements that are constantly present in steels, and it significantly influences the composition and character of non-metallic inclusions.

In the development of high-damping alloys, one of the main criteria is the unacceptable significant reduction in strength properties. Therefore, one of the reasons for choosing chromium, manganese, and vanadium as alloying elements in iron-carbon alloys was that among the main alloying elements (most commonly used), these elements more strongly strengthen ferrite than others [14].

When using alloying elements in high-damping alloys, reducing the noise level can be achieved in the case of obtaining a real research result because different classes of materials absorb sound energy of vibrations differently, depending on external factors such as the structure component ratio, type of technological processing, etc. Information that the chemical composition of alloys affects damping properties enables the development of compositions from low-alloy steels with high damping properties. In research on noise and vibration reduction during the collision of mechanism parts, noise level reduction is achieved by changing the chemical composition, type of heat treatment, increasing the mass of colliding bodies, and the duration of body collision. However, the surface of metallic materials is rarely changed [15].

The damping ability of the metallic matrix depends on the presence of microplastic deformation in its structure, which is associated with its structure and mechanical parameters. Maximum damping occurs when the structure is ferritic, while minimum damping is provided by a pearlitic structure. A mixed structure exhibits intermediate properties. A mixture of ferrite with troostite demonstrates inferior qualities compared to pearlitic, attributed to the presence of ferrite in its composition. Quenched steel with a martensitic structure dampens more strongly than troostitic due to the increased dislocation density and the appearance of residual stresses at the ends of martensitic crystals.

The use of damping non-metallic materials is limited due to their insufficient strength characteristics in most technological processes. Therefore, the question of creating iron-based alloys with increased damping capacity through changes in chemical composition and special heat treatment is highly relevant. However, the modification of structural materials by coating application is extremely rare.

Improving the operational characteristics of products by applying standard types of coatings, such as chroming and nitriding, has nearly exhausted its possibilities today, necessitating innovative approaches to improvement and the development of a new generation of functional coatings with increased resistance to destruction under conditions of cyclic thermomechanical loads and aggressive environments. One direction in this work is the creation of nanostructured coatings. Nanostructured materials with high grain boundary area exhibit high viscosity and resistance to initiation and propagation of "brittle" cracks, enabling them to resist destruction for extended periods under complex external conditions. The design of the new generation of nanostructured composite coatings with a high grain boundary area allows for the specification of a complex of high physical and mechanical properties.

Nanostructured protective coatings applied to the surfaces of mechanisms and assemblies extend the service life of equipment. Therefore, the application of nanoparticle coatings to products is an urgent task, which this work is dedicated to solving.

In industry, protective coatings are necessary to improve the performance characteristics of components, namely to increase their operational lifespan and reduce production costs. When improving the surface properties of components, their internal structure is not the determining factor. Laboratory research has shown that nanostructured coatings exhibit phenomenal surface protective properties [16-18].

The transition from micro- to nanostructured coatings allows for the enhancement of their properties due to changes in the properties of the crystalline formation itself. This results in the formation of a branched structure of grain boundaries within the film, as the number of atoms inside and on the surface of nanocrystals is equal, eliminating dislocations and internal stresses. The distance between nanocrystals equals the size of several monolayers, resulting in the quantum interaction effect.

Among the methods for forming nanostructured coatings, one of the promising approaches is the process of vacuum arc ion plasma deposition, known in global practice as the arc-PVD process.

Physical vapor deposition from the gas phase, or vacuum deposition, is a group of methods for obtaining coatings where the atomic flux of the deposited substance, created in vacuum or as a result of atomization of the surface atoms of the original material due to physical processes of material evaporation, is formed by bombardment with accelerated ions or neutral atoms.

The formation of the coating occurs as a result of a series of complex physicochemical processes: conversion of the initial deposited material into a flux of sputtered atoms; propagation of the flux towards the deposition surface; collision of the flux with the surface, followed by subsequent adsorption or desorption of atoms on it; surface diffusion of atoms to preferred nucleation sites of the coating; migration, coalescence, and growth of nuclei; coalescence of islands into a continuous film, subsequent growth of the continuous film, and formation of a coating of the required thickness. Each of these stages can be characterized by a set of parameters that ultimately determine the functional purpose of the deposited coatings and their operational characteristics. The fundamental diagram of the vacuum arc spraying method is shown in figure below [19].

The advantages of the method include the following: high coating growth rate (up to 1-1.5 μm, depending on the sprayed material and vacuum chamber configuration); the ability to control the composition of the coating by simultaneously using multiple cathodes or a single multi-component cathode; high adhesive strength of the coatings.

One of the most significant drawbacks of the method is the presence of a droplet phase in the particle stream reaching the surface of the products, which typically adversely affects the film properties and limits the method's application. This problem is addressed using arc filtration [20-21].

2. Materials and methods

For the investigations, samples of steel 20KhN (20ХН), 20KhN4PhA (20ХН4ФА), 25Kh2NMPhA (25Х2НМФА), and samples of smelted steels EO3, EO4, EO5 were used as the base. Metallic charge materials included scrap metal, ferroalloys, waste from our own production, and iron-armco.

The melting process utilized a crucible induction furnace by Reltex. The arrangement scheme of the samples for the experiment and the melting furnace is demonstrated in Figure 1. Purified titanium in the form of alloy VT1-0 with 99.5% Ti content, copper in the form of alloy M3 with 99.5% Cu content, and composite materials of the titanium-copper system, developed using the powder metallurgy method, were used as cathode materials. The saturation of the composites with the additional component (copper) was low.

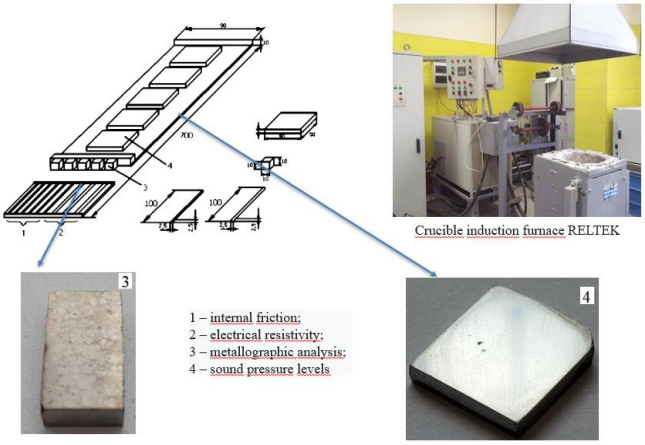

Figure 1. Scheme of cutting out the investigated samples

To implement the main aspects of forming multifunctional coatings, a special vacuum arc plasma spraying setup «Bulat» NNW-6.6-I3 (at the National University of Science and Technology «MISIS», Moscow) was used on the working surfaces of the steel. The principle of operation of the universal vacuum arc setup is provided. The resulting ceramic-metal coatings TiN-Cu with crystallite size ranging from 10 to 100 nm were obtained using ion-plasma vacuum-arc deposition.

The development stages of the ceramic-metal coatings on the surfaces of the steel samples were as follows:

- preparatory;
- ion cleaning and heating;
- application of coatings;
- cooling of the products.

The principle of operation of the universal vacuum arc setup is depicted in Figure 2.

The equipment performs the separation of neutral particles into a micro droplet phase. This is achieved by deflecting charged particles of the ion flow with a powerful magnetic field. The separator can simultaneously serve as a plasma flow accelerator, an electron source needed for thermal activation of the tool, and a source of highly charged ions of gas (nitrogen) for stimulated thermochemical treatment of the tool.

Based on the research of setups for studying acoustic (sound level, sound pressure level) and vibration (vibration acceleration level, overall vibration acceleration level) characteristics of steels, a device for comprehensive study of acoustic and vibration properties of plate and tubular steel samples was applied with further modernization [23]. The operation scheme of the setup is provided in Figure 3.

The impact ball 6 was installed on the inclined plane 5, along which it rolled down and freely fell into the geometric center of the plate sample 3. The impact ball 6 rebounds from the plate sample and lands in the ball receiver 11.

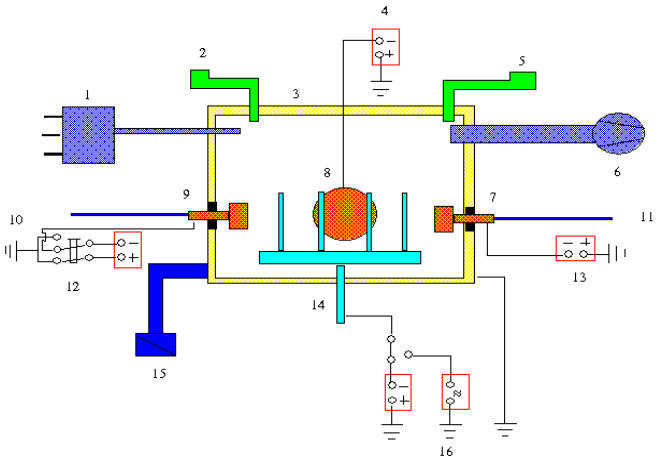

Figure 2. Scheme of vacuum arc setup [22]: 1 - gas mixer; 2 - vacuum meter; 3 - chamber of the setup; 4 - power source for the accelerator-separator; 5 - temperature control system; 6 - vacuum system; 7, 9 - arc evaporators; 8 - source of separated plasma; 10, 11 - evaporator cooling systems; 12, 13 - evaporator power sources; 14 - rotary table for tool placement; 15 - heating and cooling system of the chamber; 16 - source of pulsed bias voltage for the tool

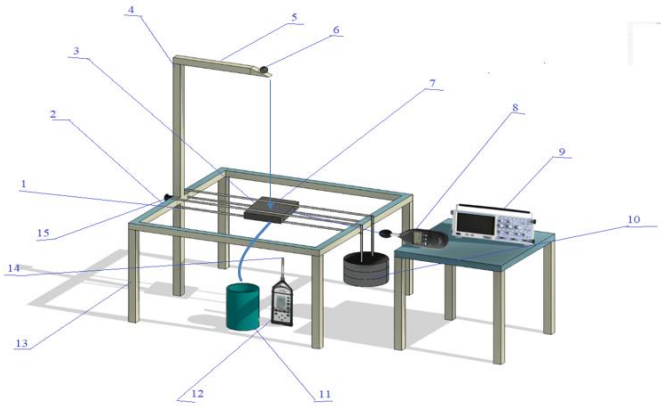

Figure 3. Device for comprehensive study of acoustic and vibration properties of solid samples [23]: 1 - nylon threads; 2 - frame; 3 - plate sample; 4 - frame stand; 5 - inclined plane; 6 - impact ball; 7 - vibration sensor of the «Bruel&Kjer» sound level meter; 8 - «Bruel&Kjer» sound level meter model 2204 with octave filter model 1613; 9 - oscilloscope C-18; 10 - weight; 11 - ball receiver; 12 - «Octava 101A» sound level meter; 13 - frame stands; 14 - microphone of the «Octava 101A» sound level meter; 15 - screw for mounting the impactor stand

Sound generated as a result of the impact between the impact ball 6 and the sample 3 is recorded using the «Octava-101A» sound level meter 12. The plate sample 3, when vibrating in the nylon threads 1, causes vibration, which is measured by the apparatus model 2204 by «Bruel&Kjer» 8. The tension of the sample with nylon threads 1 remains stable because the weight 10 controls the tension force. The height of the ball drop is adjusted by the screw for mounting the impactor stand 15. The complex of mounting the sample 3 and the impact ball 6 is fixed on the frame 2, which is secured by stands 13 at the required height above the floor.

To perform measurements, impact balls ShKh15 (IIIX15) made of steel with diameters of 7 mm (1.40 g), 8 mm (2.09 g), 9 mm (2.97 g), and 11 mm (5.55 g) were utilized. The investigation of steel plate samples (50x50x5 mm) was conducted using the setup.

The mass of the ball, the density of the sample, the distance from the impact point to the sample, and the thickness of the sample are interrelated by the following equation:

$$m \langle 4.6 \cdot \rho \cdot l \cdot h^2 \quad (6)$$

where m is the mass of the plate sample (g),

ρ is the density of the material of the plate sample (g/cm³),

l is the distance from the impact point to the nearest edge of the plate sample (cm),

h is the thickness of the plate sample (cm).

It is necessary for the width and length of the plate sample to exceed its thickness by 5 times. An experimental plate with dimensions of 50x50x5 mm meets these criteria.

The investigation of sound pressure levels was conducted in octave frequency bands ranging from 31.5 to 31500 Hz, and vibration acceleration levels were measured in the same frequency range. The sound level was adjusted according to the «A» scale, while the overall vibration acceleration level was adjusted according to the «Lin» characteristic. The use of the sound generator ZG-10 (ЗГ-10) was necessary for calibrating the sound signal studies. Corrections for changes in the sound signal due to atmospheric pressure were made using the pistonphone of the PF-101 model. The laboratory maintained a constant air temperature and humidity. Acoustic measurements were calculated as the arithmetic mean of five measurements.

Mathematical processing of the experiment results and identification of additional intervals were conducted according to the methodology. Before commencing work, the measurement setup was calibrated by verifying the sound pressure levels of the reference sample.

The determination of the dissipative properties of steels involved registering the sound impulse generated by the collision of the test sample with the striker using a recording oscilloscope. Subsequently, photographs were taken to identify damping parameters, including the logarithmic decrement, sound decay rate, relative scattering, and internal friction.

Figure 4 demonstrates a fixed photograph of the sound impulse resulting from the collision of 20KhN (20ХН) steel samples.

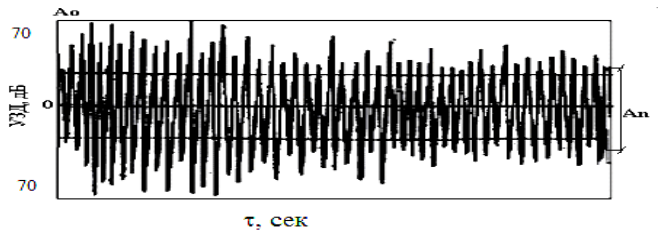

Figure 4. Oscillogram of the sound impulse decay from the collision of the 20KhN (20XH) steel sample and the impact ball

The logarithmic decrement of this alloy, δ, was determined using the following equation [24]:

$$\delta = \frac{1}{n} \ln \frac{A_0}{A_n} = \frac{1}{40} \ln \frac{74}{42} = 0.0134 \quad (7)$$

where A_0 is the initial maximum amplitude of the sound impulse,

An is the final minimum amplitude of the sound impulse,

n is the number of impulses on the oscilloscope screen.

The relative scattering, ψ, is calculated as follows:

$$\psi = 2\delta = 2 \cdot 0.0134 = 0.028 \quad (8)$$

Internal friction Q^{-1} was calculated using the following relation [25]:

$$Q^{-1} = \frac{\delta}{\pi} = \frac{\psi}{2\pi} = \frac{0.0134}{3.14} = 0.38 \cdot 10^{-2} \quad (9)$$

The time interval of the oscilloscope display is equal to 0.005 seconds. The interval is divided into 9x5=45 subintervals. Thus, the time interval division value of the oscilloscope is 0.00011 seconds.

Measurement of internal friction was conducted not only through theoretical calculations. Knowing that there is excitation of bending waves in the plate during impact, the study of internal friction of the developed alloys was carried out using the bending oscillation method. For this purpose, an automatic device was used for continuous registration of internal friction occurring during bending oscillations of rods with electromagnetic excitation in the high-frequency range (950-1000 Hz), amplitudes of 104, and temperatures ranging from 20 to 600°C.

The investigation of internal friction was conducted using a discriminator and a pulse counter according to the formula [24]:

$$Q^{-1} = \frac{\delta}{\pi} = \frac{1}{\pi \cdot n} \ln \frac{V}{V_n}, \quad (10)$$

Where δ is the logarithmic decrement; V is the initial amplitude; V_p is the final amplitude; n is the number of oscillations performed by the sample in the range from the initial to the final amplitude.

The detection of instrumental losses was carried out using a quartz rod installed in place of the sample. Such measurements allow for an assessment of the background level of the setup, which has readings of less than 10^-5, significantly lower than the minimum attenuation of the samples under investigation. A detailed description of the methodology is provided in the paper. The parameters of internal friction were studied using samples with dimensions of 1.5x1.5x100 mm after hot rolling in the frequency range of 950-1000 Hz at room temperature (20°C). Each sample was measured five times [26].

3. Results and discussion

The identification of chemical elements used in steel production and their physical parameters was carried out using commonly accepted methodologies for identifying alloying substances, as well as tensile testing methodology. The results of studying the chemical substances and physical characteristics of standard steels 20KhN (20ХН), 20KhN4PhA (20ХН4ФА), 25Kh2NMPhA (25Х2НМФА) are demonstrated in Table 1. After reviewing Table 1, you can see the results of the study of the chemical elements included in the prepared steel, as well as the physical qualities.

A comparative analysis of the data presented in Table 2 shows that the smelted steels EO3, EO4, and EO5, with comparable plastic properties (such as relative elongation δ5 and relative contraction ψ), exhibit higher strength and impact toughness indicators than standard counterparts.

Table 1. Chemical substances and physical characteristics of steels

Type of steel	Chemical elements, %								Physical qualities				
	C	Ni	Mn	Si	V	Cr	Fe	Other substances	σ_B	σ_T	Δ_s	ψ	KCU
									MPa		%		D_{zh}/sm^2
20KhN (20XH)	0.17-0.23	1.00-1.40	0.40-0,70	0.17-0.37	-	0.45-0.75	rest	≤0,035 S; ≤0,035 P; ≤0,30 Cu;	780	590	11	40	66
20 KhN4PhA (20XH4ΦA)	0.17-0.24	3.75-4.15	0.25-0.55	0.17-0.37	0.10-0.18	0.70-1.10	rest		880	685	9	40	83
25Kh2NMPhA (25X2HMΦA)	0.23-0.27	1.30-1.60	0.40-0.70	0.17-0.35	0.05	1.80-2.20	rest		657	520	14	40	49

Table 2. Chemical composition and mechanical properties of smelted steels

Type of steel	Chemical elements, %								Physical qualities				
	C	Ni	Mn	Si	V	Cr	Co	Fe	Other substances	σ_B	σ_T	Δ_s	ψ	KCU
										MPa		%		D_{zh}/sm^2
EO3	0.22	1.2	0.7	0.30	0.35	0.8	0.1	rest	0,035 S; 0,035 P; 0,35 Cu; 0,02 = Al0,01 = Bi	1100	980	11	48	120
EO4	0.35	2.5	0.8	0.20	0.40	0.8	0.2	rest		1050	950	10	45	100
EO5	0.45 - 0.48	1.0 - 1.2	0.7-0.8	0.5-1.2	0.35-0.45	0.9	0.3-0.4	rest		1100	1000	8	40	110

For instance, the yield strength (σv) of these alloys is 1.19-1.25 times greater than that of the most durable standard analogue, 20KhN4PhA (20XH4ΦA), the tensile strength (σt) is 1.39-1.46 times greater, and the impact toughness (KCU) is 1.20-1.33 times greater. These results were achieved through additional alloying of the steel with small additions of Co and increased amounts of V, as well as optimization of the content of C, Ni, Cr, Si, and Mn. Therefore, it is more promising in the present study to investigate steels based on chromium, nickel, and vanadium.

The obtained coatings had a thickness of 2.5 μm 7. The fracture of the coating exhibits signs of ductile failure and is accompanied by the formation of pits in a fibrous-striated fracture on the micro-relief (Figure 5). Analysis of the coating structure conducted using TEM demonstrates the presence of a nanostructure (Figure 5a, b).

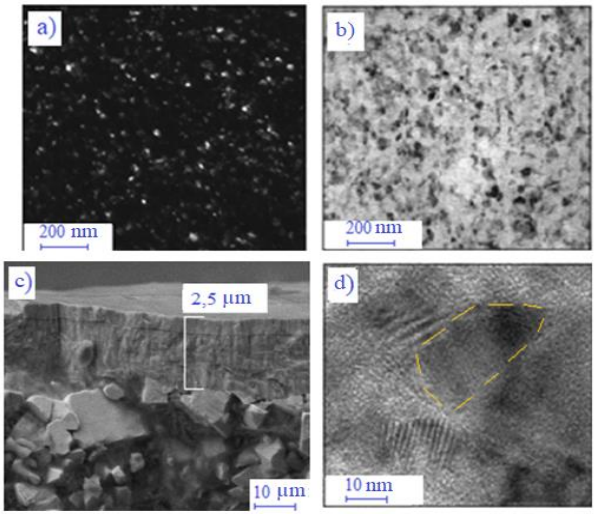

Figure 5. a) Dark-field TEM image of the coating; b) Bright-field TEM image of the cross-section of the coating; c) cross-section fracture Bright-field of TiN-Cu coating on EO5 substate; d) High-resolution TEM image of TiN-Cu coating

Based on the obtained dark-field images, it can be concluded that the obtained coatings have an average grain size of about 15-30 nm and are characterized by a layer thickness comparable to the grain size.

Figures 6-8 show oscillograms depicting the decrease in the level of the acoustic impulse against the background of the contact of a metal sphere with samples of well-known 25Kh2NMPhA (25X2HMΦA) and synthesized samples (EO5). In Figures 6-8, it can be observed based on the oscillograms of the acoustic impulse attenuation resulting from contact with a metal sphere with widely used steel grades.

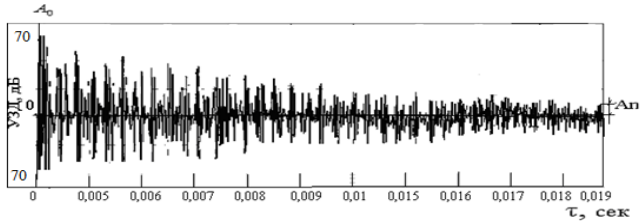

Figure 6. Oscillogram of the attenuation of the acoustic impulse from contact with a metal sphere with the reference 25Kh2NMPhA (25X2HMΦA) sample

In Figure 7, the oscillogram of the attenuation of the acoustic impulse from contact with a metal sphere with the synthesized steel EO5 is visible.

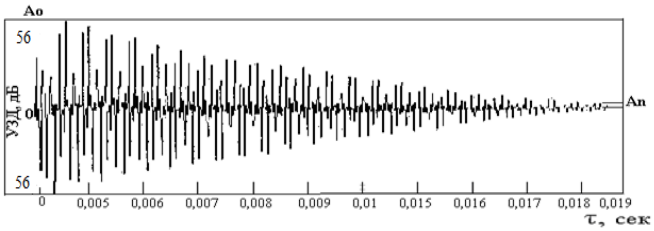

Figure 7. Oscillogram of the attenuation of the acoustic impulse from contact of a metal manufactured EO5 steel

In Figure 8, oscillograms of the attenuation of the acoustic impulse from contact of a metal sphere with EO5 (KMNC) are demonstrated, through which dissipation parameters were identified.

The oscillograms of dissipative alloys EO5 and EO5(KMNC) in terms of sound impulse attenuation show a rapid decrease in sound level, remaining within the range of 25-35 dBA over a large time interval. Meanwhile, the initial sound level is 54-56 dBA.

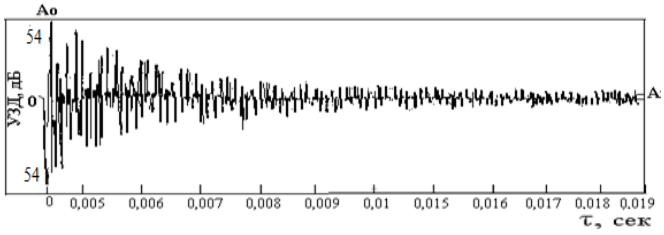

Figure 8. Oscillogram of the attenuation of the acoustic impulse from contact with a metal sphere of the smelted sample EO5(KMNC)

This indicates that the nature of sound wave dissipation in samples EO5 and EO5(KMNC) is higher than that of standard samples 25Kh2NMFA (25Х2НМФА), where the initial sound level is 77 dBA. After half of the time interval, the sound impulse decreases by half, but complete sound attenuation does not occur within 2 ms.

According to the analysis of the oscillograms of sound impulse attenuation shown in Figures 7 and 8, it can be observed that the developed alloys EO5 have the following characteristics: EO5 $Q^{-1}=1.54\cdot10^{-2}$; $\psi=9.66\cdot10^{-2}$; $\delta=4.83\cdot10^{-2}$ и EO5(KMNC) $Q^{-1}=1.72\cdot10^{-2}$; $\psi=10.8\cdot10^{-2}$; $\delta=5.40\cdot10^{-2}$. These alloys exhibit increased sound attenuation rates and dissipative characteristics compared to standard steels such as 25Kh2NMFA (25Х2НМФА), where: 25Kh2NMFA (25Х2НМФА) ($Q^{-1}=0.58\cdot10^{-2}$; $\psi=3.64\cdot10^{-2}$; $\delta=1.82\cdot10^{-2}$).

4. Conclusions

Measurements of ultrasonic pressure have shown that the application of TiN-Cu nanostructured coating, leads to an increase in the attenuation of mechanical vibration energy. When stress amplitudes exceed the critical dislocation mobility, local deformation occurs within individual grains, leading to an increase in the decrement of oscillations. However, further increases in stress levels lead to the accumulation of free dislocations at grain boundaries, reducing their mobility and consequently decreasing the oscillation decrement. The presence of thin coatings on the surface of samples results in the formation of quasi-free dislocations and changes in stress states, thus increasing the damping level of composites.

In vacuum arc deposition, the formation of nanostructured coatings and the contact interphase zone are accompanied by saturation with a large number of point and linear defects. This enhances the damping properties of the structure due to stress fields and relaxation effects. The increase in the ability to dissipate stored elastic energy after the application of coatings primarily occurs for materials with coatings having greater interfacial boundary extension, as demonstrated by multicomponent coatings. Thus, the nanostructured TiN-Cu coating exhibits the highest damping properties.

References

[1] Mukhametzhanova, D. & Bakirbekova, A. (2023). Innovative Directions of Machine Building Development in Kazakhstan. *Economic Series of the Bulletin of the L.N. Gumilyov Eurasian National University, (4), 73–78*

[2] Abdrakhmanov, N.Kh., Fedosov, A.V., Khamitova, A.N., Badrtdinova, I.I. & Matuzov, G.L. (2021). Main aspects of vibroacoustic factors assessment. *Safety of Technogenic and Natural Systems, (3), 13-22.* https://doi.org/10.23947/2541-9129-2021-3-13-22

[3] Izmerov, N.F., Buhtijarov, I.V. & Denisov, Je.I. (2016). Ocenka professional'nyh riskov dlja zdorov'ja v sisteme dokazatel'noj mediciny. *Voprosy shkol'noj i universitetskoj mediciny i zdorov'ja, (1), 14–20*

[4] Volkova, A.A., Shishkunov, V.G., Homenko, A.O. & Tjagunov, G.V. (2018). Bezopasnost' zhiznedejatel'nosti v primerah i zadachah (Uchebnoe posobie). *Ekaterinburg: Izdatelstvo Uralskogo universiteta*

[5] Efanov, A.M. (2019). Vlijanie shumovogo vozdejstvija na zdorov'e cheloveka. *Nauka-2020, 11(36), 158-163*

[6] Liming, Yu, Yue, Ma, Chungen, Zhou, Huibin, Xu. (2005). Damping efficiency of the coating structure. *International Journal of Solids and Structures, (42), 3045-3058*

[7] Kopylov, V.I. & Antonenko, D.A. (2014). Fiziko-mehanicheskie harakteristiki i vnutrennee trenie materialov s mnogofaznymi plazmennymi pokrytijami. *Problemy tehniki, (2), 72-89*

[8] Katahara, K.W., Nimalendran, M., Manghnani, M.H. & Fisher, E.S. (1979). Elastic moduli of paramagnetic chromium and Ti-V-Cr alloys. *Journal of Physycs F: Metal Physics, 9(11), 2167-2176*

[9] Bobylev, V.N., Tishkov, V.A. & Pauzin, S.A. (2007). Jeksperimental'nye issledovanija zvukoizoljacii mnogoslojnyh konstrukcij s ortotropnym sloem. *Sbornik trudov: Akustika rechi. Medicinskaja i biologicheskaja akustika. Arhitekturnaja i stroitel'naja akustika. Shumy i vibracii. Ajeroakustika, V.3, 201-205*

[10] Chatillon Jacques. (2007). Influence of source directivity on noise levels in industrial halls: Simulation and experiments. *Applied Acoustics, 68(6), 682-698*

[11] Wang Huigang, Chen Guoyue, Chen Kean, Muto Kenji. (2006). Blind preprocessing method for multichannel feedforward active noise control. *Acoustic Science Technology, 27(5), 278-284*

[12] Panigrahi, S.N. & Munjal, M. L. (2007). A generalized scheme for analysis of multifarious commercially used mufflers. *Applied Acoustics, 68(6), 660-681*

[13] J. Zhejiang Forest, Ni Yong-zhou. (2006). Zhejiang linxueyuan xuebao. *Coll., 23(1), 112-114*

[14] Martin, M.A., Tarerro, A., Gonzalez, J. & Machimbarenna, M. (2006). Exposure – effect relationships between road traffic nouse annoyance and noise cost valuations in Valladolid, Spain. *Acoust., 67(10), 945-958*

[15] Song Lei-ming, Sun Shou-guang, Xing You-sheng, Zhang Xin-hua. (2005). Ticdao xiiebao. *Journal of China Railway Society, (6), 101-104*

[16] Lenkkeri, J.T. & Lahteenkorva, E.E. (1978). An investigation of elastic moduli of vanadiumchromium alloys. *Journal of Physics F: Metal Physics, 8(8), 1643-1651*

[17] Potehin, B.A., Lukashenko, S.G. & Kochugov, S.P. (2000). Vlijanie plazmennyh pokrytij na dempfirujushhie svojstva konstrukcionnyh. *Metallovedenie i termicheskaja obrabotka metallov, (10), 30 – 33*

[18] Kutschej, K., Mayrhofer, P.H., Kathrein, M., Polcik, P. & Mitterer, C. (2004). A new low friction concept for Ti1-xAlxN based coatings in high temperature applications. *Surface and Coatings Technology, (188–189), 358 – 363*

[19] Gleiter, H. (1993). Mechanical Properties and Deformation Behaviour of Materials Having Ultra-Fine Microstructures. *Netherlands: Kluwer Akad. Publ*

[20] Pogrebnjak, A.D. Drobyshevskaja, A.A. & Beresnev, V.M. Mikro- i nanokompozitnye zashhitnye pokrytija na osnove Ti−Al−N/Ni−Cr−B−Si−Fe, ih struktura i svojstva. *Technical physics, 81(7), 124-31*

[21] Kuzmichev, A.I. (2008). Magnetronnye raspylitel'nye sis temy. *K.: Avers*

[22] Utepov, E.B., Suleev, D.K. & Utepov, T.E. (2000). Nauchnye osnovy sozdanija «tihih» splavov (problemy akustiche-skoj jekologii). *Almaty: LLP «Print»*

[23] Granato, A., Lucke, K. (1956). Theory of Mechnical Damping Due to Dislocations. *Journal of Applied Physics, 27(6), 583-593*

[24] Cremer, H. & Cremer, L. (1948). Theoride der Entstehung des klopts – chalts. *Erequenz1948, 2(3), 61-71*
[25] Kerzhencev, V.V. & Dedenko, L.G. (1971). Matematicheskaja obrabotka i oformlenie rezul'tatov jeksperimenta. *M.: MGU*
[26] Krishtal, M.A. & Golovin, S.A. (1976). Vnutrennee trenie i struktura metallov. *M.: Metallurgija*
[27] Abuova, R.Zh. (2020). Structure of chromium-nickel vanadium steels with ceramic (TINKA) nanostructured coating to solve noise reduction problems. *Bulletin of Kazakh Leading Academy of Architecture and Construction, №3(77), 233-240.* https://doi.org/10.51488/1680-080X/2020.3-31
[28] Abuova, R.Zh, Ten, E.B., Burshukova, G. (2021). Study of vibration properties of ceramic-metal nanostructural TIN-CU coatings with different copper content 7 and 14 at. % on chromium-nickel-vanadium steels. *News of the national academy of sciences of the republic of Kazakhstan series of geology and technical sciences, 5(449), 6-13.* https://doi.org/10.32014/2021.2518-170X.92

TiN-Cu металл керамикалық наноқұрылымды жабыны бар жаңа Cr-Ni-V болаттарының жақсартылған демпферлік қасиеттері

Р.Ж. Абуова[1*], А. Бондарев[2], Г.А. Буршукова[3]

[1]*Халықаралық білім беру корпорациясы, Алматы, Қазақстан*
[2]*Лимерик Университеті, Ирландия*
[3]*Satbayev University, Алматы, Қазақстан*

**Корреспонденция үшін автор: ryskena@mail.ru*

Аңдатпа. Бұл мақалада демпферлік қасиеттері жоғарылаған композициялары бойынша құрамында Cr, Ni, V қоспалары бар жаңа балқытылған болаттарды жасау және оларды наноқұрылымды жабындарды тұндыру арқылы олардың демпферлік қасиеттерін одан әрі арттыру тәсілі ұсынылды. Балқытылған жаңа ЭО5 болаттарға иондық-плазмалық вакуумды-доғалық тұндыру әдісі арқылы (TiN)-Cu жабындардың құрылым және фаза түзілу процестерін зерттеу нәтижелері берілген. Қаптаманың сынуы иілгіш сыну белгілеріне ие және микрорельефте талшықты жолақты сынық шұңқырларының пайда болуымен бірге жүреді. Бөлшектердің сипатына сүйене отырып, ығысу кернеулері бұзылуға негізгі үлес қосады деп болжауға болады. Жүктеме ұлғайған сайын жабындар негізінен сызаттың жиегі бойынша бұзылады, яғни жабынның субстрат материалына көбірек шегінуі кезінде сызаттың шеттеріндегі қысу және созылу кернеулері бұзылуда маңызды рөл атқара бастайды. Бұл зерттелетін жабындардың нанокомпозиттік құрылымымен түсіндіріледі, ол шекаралардың тармақталған желісінің әсерінен жарықшақтардың таралуын тежеуге, сондай-ақ тұтқырлықты сақтауға көмектеседі. Микродифракциялық талдау және қараңғы өрістегі ТЕМ кескіндері негізінде жабындағы кристаллиттер титан нитриді δ-TiN болып табылады деп қорытынды жасауға болады; жабындарда кристаллографиялық құрылым анықталмады. TiN фазасының кристаллит өлшемі TiN-Cu жабыны бар болат үлгілерінің ішкі үйкелісінің амплитудалық тәуелділіктерін құрайды. Демпферлік сипаттамалардың болуы наноөлшемді TiN түйіршіктерінің шекарасында керамикалық негізден және мыс пластикалық фазасынан тұратын жабынның композициялық микроқұрылымына байланысты. Жабындардың өзіне және субстратқа бөлек тән ішкі демпферлік сипаттамаларға қосымша «жабын-негіз» интерфейсінде қосымша демпферлік механизмдер жүзеге асырылады.

Негізгі сөздер: *наноқұрылым, демпферлеу, дислокация, микроқұрылым, шу, діріл, шу өлшегіш.*

Улучшенные демпфирующие свойства новых сталей Cr-Ni-V с металлокерамическим наноструктурным покрытием TiN-Cu

Р.Ж. Абуова[1*], А. Бондарев[2], Г.А. Буршукова[3]

[1]*Международная образовательная корпорация, Алматы, Казахстан*
[2]*Университет Лимерик, Ирландия*
[3]*Satbayev University, Алматы, Казахстан*

**Автор для корреспонденции: ryskena@mail.ru*

Аннотация. В данной статье проведены исследования впервые разработанных составов сталей марки ЭО5, легированных Cr, Ni, V, обладающими повышенными демпфирующими свойствами и предложен подход по дальнейшему повышению их демпфирующих свойств за счет осаждения на их поверхность покрытий. Приведены результаты исследований процессов формирования структуры и фазообразования в покрытиях (TiN)-Cu полученных методом ионно-плазменного вакуумно-дугового напыления на подложки из выплавленных сталях ЭО5. Излом покрытия имеет признаки вязкого разрушения и сопровождается образованием ямок волокнисто-полосчатого излома в микрорельефе. Исходя из характера отслоений при скратч-тестировании, можно предположить, что основной вклад в разрушения

вносят сдвиговые напряжения. При увеличении нагрузки покрытия основном разрушаются по краю царапины, то есть при большем вдавливании покрытия в материал подложки существенную роль в разрушении начинают играть сжимающие и растягивающие напряжения по краям царапины. Это объясняется нанокомпозиционной структурой исследуемых покрытий, способствующей сдерживанию распространения трещин за счет разветвленной сети границ, а также сохранения вязкости. По микродифракционному анализу и полученным темнопольным изображениям методом ПЭМ можно заключить, что кристаллиты в покрытии являются нитридом титана δ–TiN, кристаллографической текстуры в покрытиях обнаружено не было. Размер кристаллитов фазы для TiN составляет амплитудные зависимости внутреннего трения образцов сталей с покрытиями TiN-Cu. Наличие демпфирующих характеристик обусловлено композиционной микроструктурой покрытия, состоящей из керамической основы и пластичной фазы меди по границам наноразмерных зерен TiN. Кроме внутренних демпфирующих характеристик, присущих самим покрытиям и подложке по отдельности, реализуются дополнительные демпфирующие механизмы на границах раздела «покрытие-основа».

Ключевые слова: *наноструктура, демпфирование, дислокация, микроструктура, шум, вибрация, шумомер.*

Received: 25 November 2023
Accepted: 15 February 2024
Available online: 29 February 2024